RAL-88-056

Science and Engineering Research Council
Rutherford Appleton Laboratory
Chilton DIDCOT Oxon OX11 0QX

RAL-88-056

Measurement of the Spin-rotation Parameter, β, in the Reaction $\pi^+ p \rightarrow K^+ \Sigma^+$ at 1.69 and 1.88 GeV/c

D J Candlin et al

June 1988

MEASUREMENT OF THE SPIN-ROTATION PARAMETER, β, IN THE REACTION $\pi^+p \to K^+\Sigma^+$ AT 1.69 AND 1.88 GeV/c

D J Candlin, D C Lowe and K J Peach
Department of Physics, University of Edinburgh
Edinburgh, UK

C J Brankin, I F Corbett, S M Fisher, G S Ioannidis,
P J Litchfield, L P Mapelli[1], J Wright
Rutherford Appleton Laboratory, Chilton, Didcot, Oxon, UK

M G Green
Department of Physics, Royal Holloway and Bedford New College,
Egham Hill, Egham, Surrey

E. Arik[2], G D Hallewell[3], B Pollock and A Shirani
Department of Physics, Westfield College, London UK

Abstract

Values of the spin rotation parameter, β, are measured in the reaction $\pi^+p \to K^+\Sigma^+$ at incident pion momenta of 1.69 and 1.88 GeV/c.

Present Address

1) CERN, 1211 Geneva 23, Switzerland
2) Bogazici University, Bebek, Istanbul, Turkey
3) SLAC, P O Box 4349, Stanford, California, USA

1) Introduction

This paper presents the results of a measurement of the spin rotation parameter, β, in the reaction $\pi^+ p \rightarrow K^+\Sigma^+$ at two incident pion momenta, 1.69 and 1.88 GeV/c. The experiment was run at the CERN PS using the Rutherford Multiparticle Spectrometer (RMS). It was a follow-up to the experiment performed at NIMROD in which the differential cross-sections and polarisations were measured at 26 momenta between 1.282 and 2.473 GeV/c[1].

A partial wave analysis of the earlier data was carried out,[2] yielding parameters for Δ^* resonances formed in this reaction. The objective of this second experiment was to add qualitatively new information to the partial wave analysis by measuring the spin rotation parameter, the only other observable available in this reaction, at a few points in the above energy range. In principle, the measurement of β at a momentum point resolves many of the mathematical ambiguities present in the partial wave analysis which in reference 2 were only resolved by continuity and the imposition of resonance behaviour in certain dominant partial waves.

As its name implies the measurement of β involves the correlation of the initial spin of the target proton with the outgoing spin of the Σ^+. The initial spin direction was defined by the use of a frozen spin polarised target yielding average polarisations of the order of 95% for free protons. The outgoing Σ spin direction was measured using the weak decay of the Σ^+ into $p\pi^0$. This experiment is the first to attempt to measure the β parameter in this reaction. The only comparable data is the measurement of the same parameter in the reaction $\pi^- p \rightarrow K^0\Lambda^0$[3].

2) Experimental Conditions

2.1 Rutherford Multiparticle Spectrometer

RMS was a large dipole magnet (4m x 2m x 1.35m) equipped with tracking detectors and trigger counters, originally built to study complex reactions in the energy range available at the NIMROD accelerator at the Rutherford Laboratory. The detector layout used in the previous experiment at NIMROD is described in some detail in reference 1. It consisted of a set of cylindrical spark chambers surrounding the target, a set of downstream flat spark chambers, a set of flat spark chambers to one side of the target to measure slow positively charged tracks that curve in that direction, a set of multiwire chambers to define the momentum and direction of beam particles, time of flight and trigger scintillation counters behind the two sets of flat chambers and a downstream high pressure cherenkov counter that vetoed pions above about 1.3 GeV/c. This layout had a high acceptance for $K^+\Sigma^+ \rightarrow K^+p\pi^0$ final states produced in the plane of the magnet and proved very successful in being able to reconstruct fully the $\Sigma^+ \rightarrow p\pi^0$ decay and separate this reaction from the possible backgrounds.

Several minor changes, detailed below, were made for the second stage of the experiment:

a) The magnet was modified by the addition of carefully shimmed pole pieces which provided the 2.5 T field, uniform over the volume of the target to ±.4 mT, required to polarise the target uniformly.

b) The side spark chambers were replaced with proportional chambers (SD1-4).

c) Two proportional chambers were placed behind the large downstream hodoscope (DS1, DS2).

d) The first downstream flat spark chamber was replaced by a proportional chamber (MD1).

e) A 20cm square proportional chamber was placed after the cylindrical chambers (U1).

f) The downstream hodoscope, J1 was raised so that the bottom element was centred on the incident beam. The downstream cherenkov was raised to cover the same aperture.

The layout for this experiment is shown in Figure 1.

The objective of the changes was to provide extra triggering capability using the MWPC, since the trigger for the first part of the experiment was not appropriate for the spin rotation measurement, and also to provide some increased track point accuracy and efficiency.

2.2 The beam

It was originally proposed to run both the hydrogen target and polarised target experiments at NIMROD. However on the closure of NIMROD the equipment was moved to CERN and installed in the East Hall at the PS. A conventional separated beam with one stage of electrostatic separation provided approximately 10^5 positive pions per pulse of a few hundred milliseconds duration. The proton contamination was very small but the identification of the beam particle was confirmed by a time-of-flight measurement over 13m with an accuracy of ± 250 psec. The electron and muon contaminations were separately measured. The beam would provide pions from 1.3 to 2.5 GeV/c but good data were obtained at only two momenta, 1.69 and 1.88 GeV/c.

2.3 Trigger

The dipole configuration of the magnet is not ideal for a spin rotation measurement as the maximum effect occurs when the polarisation direction, which is aligned with the magnetic field, lies in the event production plane (See Section 4.1). The trigger was designed to select events which could be fully reconstructed in the detector and approached as closely as possible the desired orientation. This goal could best be realised in two limited kinematic regions; the "forward" region ($0.7 < \cos\theta < 1.0$) and the "backward" region ($-0.9 < \cos\theta < -0.1$) where $\cos\theta$ is the centre of mass scattering angle of the K^+.

The forward trigger demanded a correlation in the bending plane between the coordinates of a track in MWPC U1 and DS1 based on the known kinematics of the K^+. As well as these forward K^+ events this trigger also accepted an appreciable fraction of the protons from backward $K\Sigma$ events which have a similar momentum/angle correlation.

The backward trigger demanded a track in the backward part of the first side MWPC (SD1) plus a forward track in U1 and DS1 but without requiring the correlation in position in the two chambers. In addition any hits in the regions of MD1 not covered by U1 and in the forward part of DS1 vetoed the event.

Both triggers required a count in the hodoscope J1 and no count in the cherenkov counter, thus vetoing pions over 1.3 GeV/c momentum. The presence of a good beam particle was imposed by scintillation counters and solid state counters in the beam.

2.4 Polarised target

A frozen spin target 12cm long and 1cm radius made of propanediol ($C_3O_2H_8$) was used, giving a free to bound nucleon ratio of 1:9.5. Two NMR coils around the target measured the target polarisation.

The target was polarised in a field of 2.5T at a temperature of about 1K between the shimmed pole pieces added to the RMS magnet. Typically polarisations of 95% were achieved, determined by calibration of the NMR coils on the natural polarisation of about 0.25% produced by the polarising field alone. The target was then cooled to below 50mK and moved to its working position in the experiment where the polarisation was maintained by the 1T field of the RMS magnet. Polarisation lifetimes of typically 800 hours for positive polarisations and 330 hours for negative polarisations were obtained.

Data were taken in runs of typically 3 days between repolarisation for positive polarisations and 2 days for negative. The analysis procedure adopted (see section 4) depends on the mean +ve and -ve polarisation being equal to better than the error on the polarisation value obtained in the subsequent analysis (typically 10%). Study of the NMR measurements shows that the spread in the difference in initial polarisation measurements between positive and negative is 3%, and the difference in average polarisation due to the difference in polarisation lifetimes in the two cases 2.8%. Also the run to run stability of the polarisation measurement was found to be good to 3%.

We conclude that the positive and negative polarisations under which the experiment was run were equal to better than ± 6%.

Two solid state counters mounted in the target cryostat and operated at liquid helium temperatures ensured that the beam trajectory passed through the target material and avoided the significant mass surrounding the propanediol target.

3) Data

3.1 Data taking

Because of problems with setting up the polarised target* only one month of good data taking was available before the PS shutdown during which the East Hall was to be remodelled for LEP operations and the beam line dismantled. In this period useful data could be taken at only two momenta, 1.69 and 1.88 GeV/c. Moreover, in order to obtain the maximum data in the minimum time, only the forward trigger was run as this trigger accepted both forward and backward events, though with a reduced efficiency in the backward direction. Approximately 6×10^6 triggers were taken at each momentum point, 3×10^6 at each polarisation setting. Again in order to save time the polarisations were not reversed after each 2 or 3 day polarisation period but the polarisation was topped up to its maximum value. The polarisation was reversed after all data at one setting had been obtained; typically less than one week's running. The study described above in section 2.4, together with the powerful analysis technique available and the observation that the statistical precision available did not require high precision on the polarisation measurement, confirmed that this arrangement was adequate for this experiment, though not ideal.

3.2 Data reduction

Essentially the same data reduction programs were used as in the first part of the experiment. These are described in some detail in reference 1. Tracks with more than 4 hits were found and had their momenta and direction fitted with high efficiency (greater than 95%). Corrections for ExB and track angle effects in the spark chambers were applied and the full

---

* The original target vessel could not be used. We would like to thank the CERN polarised target group and particularly Dr T Niinikowski for the loan of a similar vessel and their help during the setting up of the polarised target.

correlated Coulomb scattering error matrix used in the fit. All pairs of outgoing tracks were subjected to a combined geometrical and kinematic fitting procedure which performed a two vertex geometrical fit to the $\pi^+p \rightarrow K^+\Sigma^+ \rightarrow K^+p\pi^0$ reaction subject to the kinematical constraints at each vertex. The decay length of the Σ^+, which was not observed in the track detectors, was a parameter of the fit.

In addition the times of flight in hodoscopes J1 and J2 (if the latter was hit) were calculated and a time of flight χ^2 added to the kinematic χ^2. Fits were also carried out for the single vertex hypotheses $\pi^+p \rightarrow \pi^+p$, $\pi^+p\pi^0$ and $\pi^+\pi^+n$.

The same cuts to separate $K\Sigma$ events from background were used as in reference 1. Studies there showed that for events produced from free hydrogen a pure sample of $K^+\Sigma^+$ events was obtained with less than 4% contamination of background events. As an indication of purity of the sample Figure 2 shows the time of flight probability for tracks that hit J2 assuming that they are π, K or p after kinematic fitting and before the final selection process. It can be seen that even at this stage the majority of events contain a good K^+.

3.3 Final event Sample

It was found that at both momenta the events entering the lower element of hodoscope J1, i.e. events whose production plane is perpendicular to the polarisation direction, contained considerably more background than those in the other two elements. Since these events had low weight for the determination of β they were rejected. Cuts to ensure good measurability of the tracks and vertex position cuts were also imposed.

Finally a selected sample of 3297 positive polarisation and 2898 negative polarisation $K^+\Sigma^+$ events remained at 1.69 GeV/c and 2748 positive and 2721 negative events at 1.88 GeV/c. The distribution in cos Θ for the two data sets is shown in Figure 3. Due to a misalignment of the trigger counters U1 and DS1, the acceptance of the forward trigger to forward $K^+\Sigma^+$ events from free hydrogen was poor. However, it had little effect on the acceptance for the backward events which was insensitive to their positioning.

3.4 Monte Carlo

As in the hydrogen target experiment a complete simulation was carried out using Monte Carlo generated, tracked and triggered events which were then passed through the identical set of reconstruction and selection programs. The details are the same as those described in reference 1. About three times as many good Monte Carlo as data events were produced. This involved the generation and tracking of approximately 0.5 million $K^+\Sigma^+$ events at each polarisation and momentum setting.

4) Data Analysis and Results

4.1 Formalism and method

The reaction $\pi^+p \to K^+\Sigma^+ \to K^+p\pi^0$ is described by 5 variables. We chose;

1) Total centre of mass energy (E).
2) Centre of mass production angle of the K^+ (θ). ($\bar{\pi}.\bar{K} = \cos\theta$ where $\bar{\pi}$ is the incident pion direction and $\bar{K}$ is the outgoing K^+ direction)
3) Angle between the polarisation direction and the event production plane projected onto the plane perpendicular to the incident π direction (ϕ).
4) 5) the polar (θ_d) and azimuthal (ϕ_d) decay angles of the proton defined in the Σ^+ decay frame such that the proton direction ($\bar{p}$) has components
$\bar{p}.\bar{n} = \cos\theta_d \quad \bar{p}.\bar{\Sigma} = \sin\theta_d \cos\phi_d \quad \bar{p}.(\bar{n} \times \bar{\Sigma}) = \sin\theta_d \sin\phi_d$
where $\bar{n}$ is the normal to the production plane ($\bar{\pi} \times \bar{K}$) and $\bar{\Sigma}$ is the Σ direction.

For a given centre of mass energy and production angle bin the distribution function is given by

$$W = 1 + \alpha P \cos\theta_d + P_T\left[P \sin\phi + \alpha\left\{\sin\phi \cos\theta_d + \sqrt{(1-P^2)}\right.\right.$$
$$\left.\left.\sin\theta_d \cos\phi \sin(\theta + \phi_d - \beta)\right\}\right]$$

where P is the Σ polarisation

P_T is the target polarisation

α is the Σ asymmetry parameter (-0.979)

β is the spin rotation parameter.

Note that P can be determined twice, once from the Σ decay and once from the polarised target term, also that a term $\alpha P_T \sin \phi \cos \Theta_d$ exists which is independent of the Σ polarisation.

The three parameters P, P_T, β can be determined by a maximum likelihood fit of the data to this expression, that is by minimising the expression

$$\frac{- \ln \left(\prod_{i=1}^{N} W_i \right)}{NA}$$

A is the integral of W weighted by the acceptance of the experiment, determined by the Monte Carlo simulation, and N is the total number of events.

A significant simplification can be made by observing that the two settings of the polarisation are equivalent to taking data with the same polarisation in regions corresponding to ϕ and $\phi + \pi$. Making the ϕ transformation in the expression for W it can be seen that all terms apart from $\alpha P \cos \Theta_d$ change sign. Thus if we analyse the two data sets as one, with the negative polarisation reversed and its ϕ transformed, then all terms in the integral A, except the $\alpha P \cos\Theta_d$ term, vanish under the assumptions:

a) that the acceptance is the same for the two polarisation settings, a good assumption for the 1.69 and 1.89 data which were taken over a short period with the equipment in a stable configuration,

b) that the distribution of background events (i.e. $K^+\Sigma^+$ events from unpolarised protons and events that are not $K^+\Sigma^+$ but that give fits and pass the selection criteria) are the same in the two polarisation settings, again a good assumption since the background from bound protons is unaffected by the polarisation setting and the analysis of reference 1 showed that the background from free protons is negligible,

c) that the free polarisation is the same in the two settings, justified in section 2.4, Since the transformed integral depends on only one variable it can be determined to a sufficient accuracy by rather modest amounts of Monte Carlo data, in contrast to the integrals involving β. Furthermore its correlation with β is small so that the determination of β is almost independent of the detailed acceptance of the experiment.

A correction has been applied to take account of the small difference (less than 10%) in the amount of data taken at the two polarisation settings by weighting the negative polarisation data by the ratio of the beam counts in the two settings. Small errors due to differences in transmission coefficients in the two settings are below the sensitivity of the experiment. Tests were made with different values of the weights, within reasonable ranges, without affecting the value of β within its errors.

4.2 Fitting procedure

The sample of selected events consists of three types

a) $K^+\Sigma^+$ events off polarised free protons

b) $K^+\Sigma^+$ events off bound protons (zero polarisation)

c) background non-$K^+\Sigma^+$ events.

Events of type b) merely dilute the effective target polarisation from the measured 95% of the free protons. Events of type c) will obviously not have the characteristics of $K^+\Sigma^+$ events and in particular, since they will generally come from events not containing weak decays will have zero or low effective Σ polarisations as measured with the $\alpha P\cos\theta_d$ term.

It might be hoped to distinguish between the free proton events and the others using the kinematic fit probability. This probability was studied for the free hydrogen data in reference 1 and found not to be flat but to be peaked to low values. This was attributed to residual misalignments of chamber positions and uncertainties in the field maps and in spark corrections. These effects are expected to remain in this data. In addition events of types b) and c) would be expected to populate the low probability region. Figure 4 shows a typical probability distribution.

Fits were made with a variable lower probability cut. The results for P and P_T are shown in Figure 5 for the 1.69 GeV/c data. It can be seen that the absolute value of P rises as the cut is increased and there is also a tendency for P_T to rise. These reflect the removal of events which are not $K^+\Sigma^+$ off free hydrogen as the probability cut is increased. A probability cut of 5% optimises the removal of background while retaining a maximum number of events. Figure 6 shows the measured Σ polarisation (P) at 1.69 and 1.88 GeV/c with this cut compared with the results obtained in the hydrogen target experiment[1]. The agreement is good, indicating that the fitting process is working well and justifying the assumptions made. Effective target polarisations of around 20% were obtained, representing the dilution of free with bound proton events.

4.3 Measurement of β

The values of β obtained with a 5% probability cut in 4 bins of cos θ at 1.69 and 3 at 1.88 are plotted in Figure 7 and tabulated in Table 1. Because of the different acceptance at the two momentum points the cos θ binning is different in order to obtain approximately equal numbers of events per bin. The data with cos $\theta < -0.7$ at 1.88 GeV/c had small values of effective target polarisation and too big errors on β to be useful. Within the quoted errors the value of β is not affected by the value of the probability cut. Figure 8 shows some sample distributions of the angle combinations involved in the expansion of the distribution function W, together with the Monte Carlo expectations given the values of the fitted parameters. Note the generally good fits; the combination sin ϕ cos θ_d is dependent only on the target polarisation (P_T), cos θ_d is dependent only on P. Notice also the broad range of the distribution involving cos $(\theta-\beta)$ (cos ϕ sin θ_d sin ϕ_d). The experiment has good sensitivity to β despite the restricted acceptance.

4.4 Comparison with the partial wave analysis

The partial waves determined in reference 2 were used to calculate the expected values of β. The formalism used in references 3 and 4 was followed. Briefly this reaction is described by a scattering matrix

$$M = f + ig\underline{n}.\underline{\sigma}$$

where f is the non-spin-flip amplitude

g is the spin-flip amplitude

$\underline{n}$ is the production plane normal

$\underline{\sigma}$ are the Pauli spin matrices

The observables I_o (the intensity for zero target polarisation), P (the polarisation) and β (spin rotation angle)[(5)] are defined in terms of f and g as

$$I_o = |f|^2 + |g|^2$$

$$I_o P = -2\ \mathrm{Im}\ (f^* g)$$

$$\beta = \arg\ \left(\frac{f-ig}{f+ig}\right)$$

$$= \tan^{-1}\ \left(\frac{-2\ \mathrm{Re}(f^* g)}{|f|^2 - |g|^2}\right)$$

f and g can be simply calculated from the partial wave amplitudes[4)].

The predictions of the partial wave analysis are plotted as the curves on Figure 7. The overall agreement of the new data and the predictions of reference 2 is not good. The χ^2 of the fit at 1.69 GeV/c is 22 for 4 data points and 5.4 for 3 data points at 1.88 GeV/c.

The Barrelet zeros formalism[(6)] has been used to calculate the 1024 ambiguities to the partial wave amplitudes determined in reference 2 at each of the two data points measured here. Amongst these ambiguities a number can be found that give good values of χ^2 for the fit of their predicted β values to these measured here. However none of them have the pattern of amplitudes in the high partial waves (F_{17} and above) that was inferred from the resonance pattern in these waves determined in the elastic channel and used in reference 2 to constrain the energy continuity of the solution. A new partial wave analysis incorporating this data is needed to determine whether a fit to β can be obtained by small adjustments around the values found in reference 2 or whether a solution corresponding to a completely different Barrelet ambiguity is required in this energy region.

5. Acknowledgements

Our thanks are due to the many people who contributed to this experiment. J Alner, J Chauhan, J Craig, D Cragg, S Cox, M Page, G Pullinger, G Warner and P White built and operated the polarised target. M Gibson, M Morrissey and R Nickson worked long and hard to keep a big experiment with a small crew on the road. Finally we would like to thank all the staff of CERN, particularly the crew of the PS, for their usual efficiency and professionalism.

References

1) D.J. Candlin et al. Nucl. Phys. B226 (1983), 1.

2) D.J. Candlin et al. Nucl. Phys. B238 (1984), 477.

3) K. Bell et al. Nucl. Phys. B222 (1983), 389.

4) D.H. Saxon and J.B. Whittaker, Rutherford preprint RL-80-076 (unpublished).

5) R.L. Kelly, J.C. Sandusky, R.E. Cutkosky, Phys. Rev. D10 (1974), 2309.

6) E. Barrelet, Nuovo Cimento A8 (1972), 331.

Table 1

Measured values of β (all values are modulus 2π)

1.69 GeV/c		1.88 GeV/c	
cos Θ range	β	cos θ range	β
− 0.9 − 0.7	− 1.4 ± 1.0		
− 0.7 − 0.4	− 0.7 ± 0.9	− 0.7 − 0.5	1.2 ± 2.1
− 0.4 − 0.1	0.9 ± 0.9	− 0.5 − 0.3	0.2 ± 1.4
0.7 0.95	− 1.9 ± 0.9	0.7 0.9	1.4 ± 2.5

Figure Captions

Figure 1 Layout of chambers and counters in the RMS magnet.

Figure 2 The time-of-flight probability for a typical sample of 213 $K^+\Sigma^+$ events selected on kinematic probability in which the backward particle entered hodoscope J2, assuming the particle is a π^+,K^+ or proton. Hypotheses with very low probabilities are not included in the plots.

Figure 3 Centre of mass scattering angle (θ) distributions for (a) 1.69 GeV/c +ve and −ve polarisations (b) 1.88 GeV/c +ve and −ve polarisations.

Figure 4 A typical kinematic fit probability distribution. The arrow shows the 5% probability cut determined in the analysis described in the text.

Figure 5 Fitted values of P_T and P for the four cos θ bins at 1.69 GeV/c as a function of the kinematic probability cut.

__Figure 6__ Values of the Σ polarisation measured in this experiment (open circles) compared with those measured on a hydrogen target in reference 1 (solid circles).

__Figure 7__ Fitted values of β plotted as a function of cos θ. The solid curve is the prediction of the partial wave analysis of reference 2.

__Figure 8__ Comparison of the data at 1.69 GeV/c, +ve polarisation, (histogram) and the distributions predicted by the Monte Carlo programme (•) assuming the fitted values of P, P_T and β and including the full experimental acceptance for (a) cos Θ_d (b) sin ϕ cos Θ_d (c) cos ϕ sin θ_d sin ϕ_d.

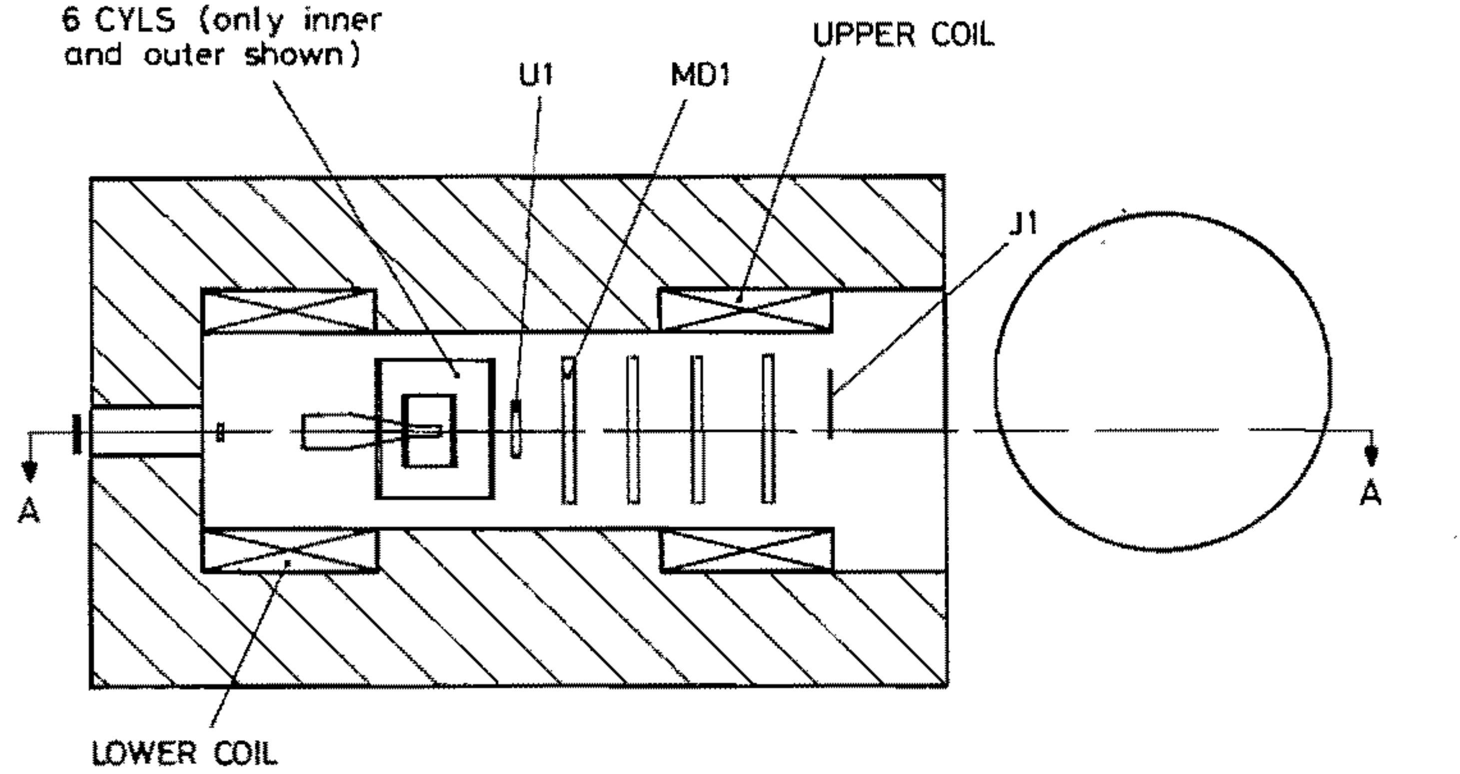

SECTION B-B (side view)

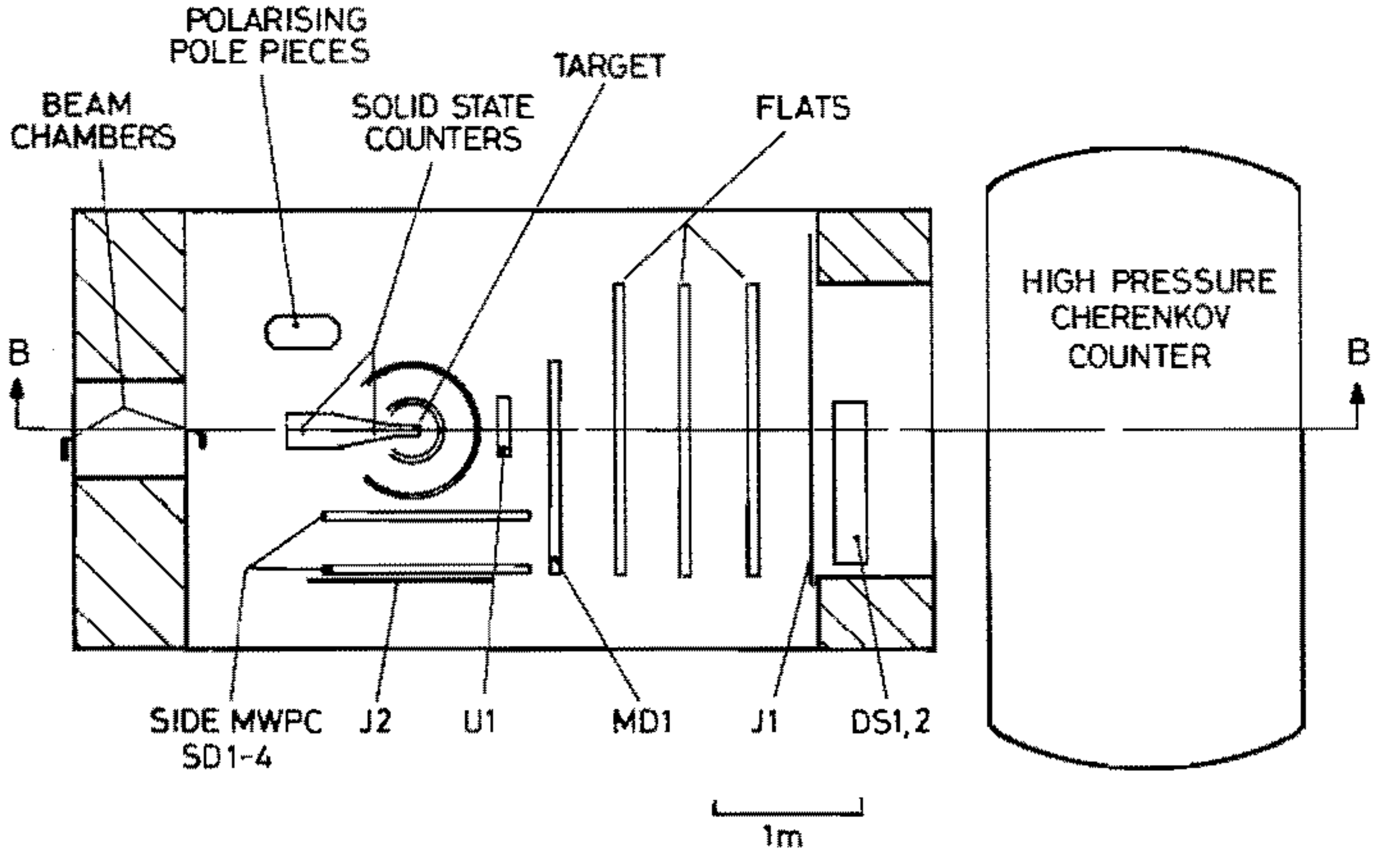

SECTION A-A (top view)

FIG. 1

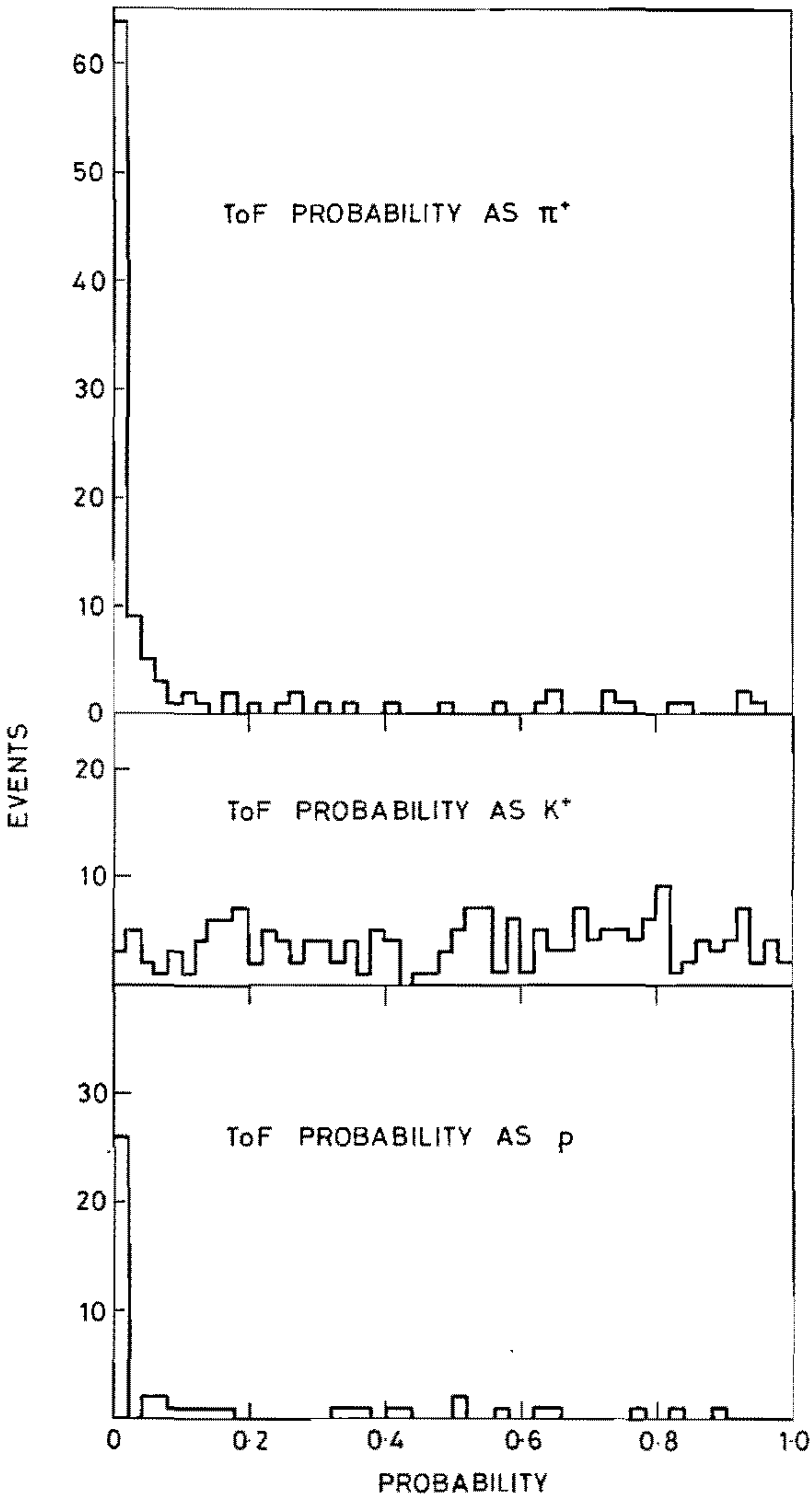
EVENTS
ToF PROBABILITY AS π^+
ToF PROBABILITY AS K^+
ToF PROBABILITY AS p
0
10
20
30
40
50
60
0.2
0.4
0.6
0.8
1.0
PROBABILITY

FIG. 2

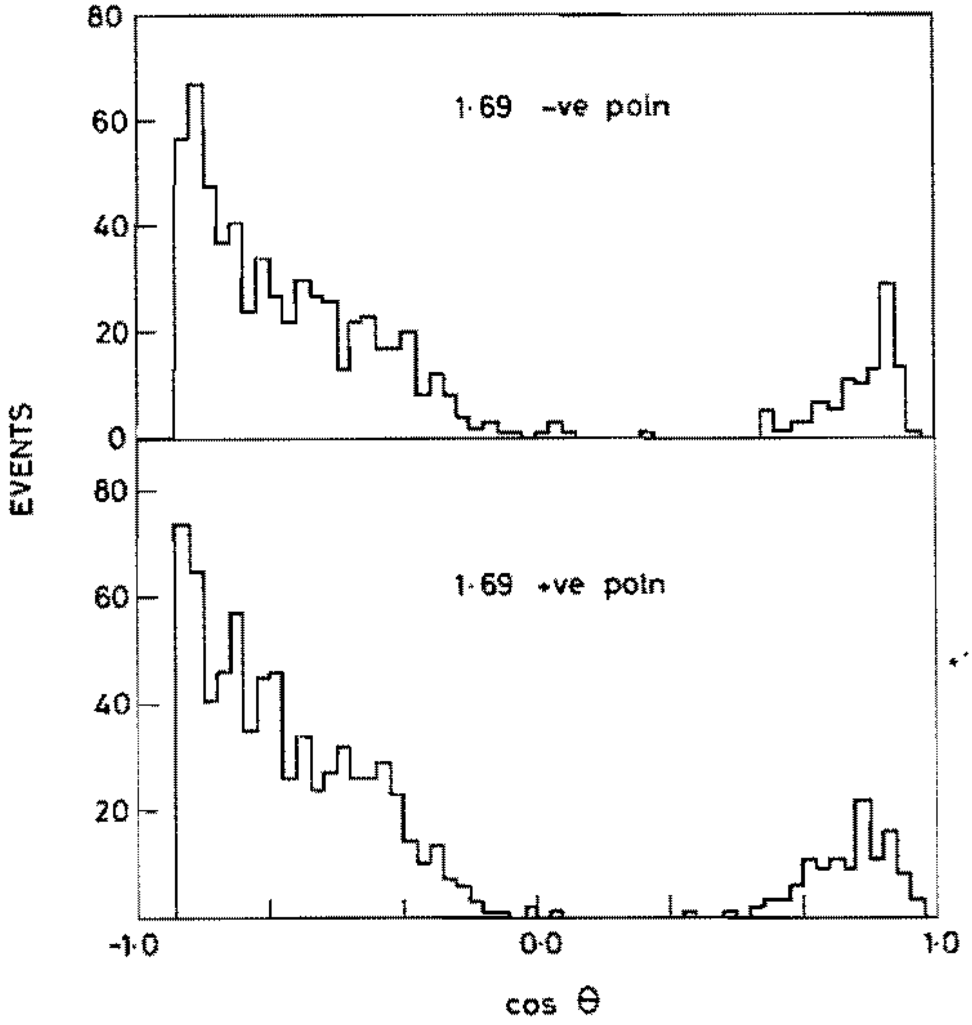

80
60
40
20
0
1·69 -ve poin
EVENTS
80
60
40
20
1·69 +ve poin
-1·0
0·0
1·0
cos θ

FIG. 3a

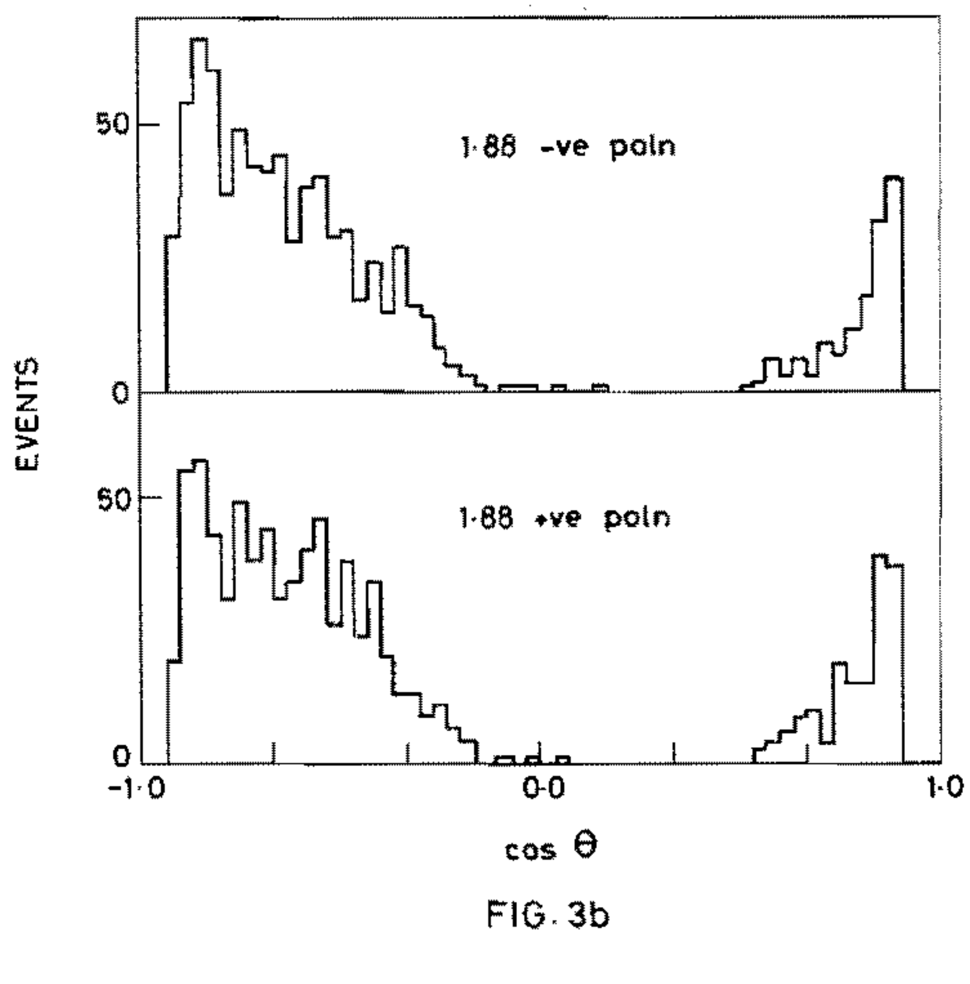

50
0
1·88 -ve poin
EVENTS
50
0
1·88 +ve poin
-1·0
0·0
1·0
cos θ

FIG. 3b

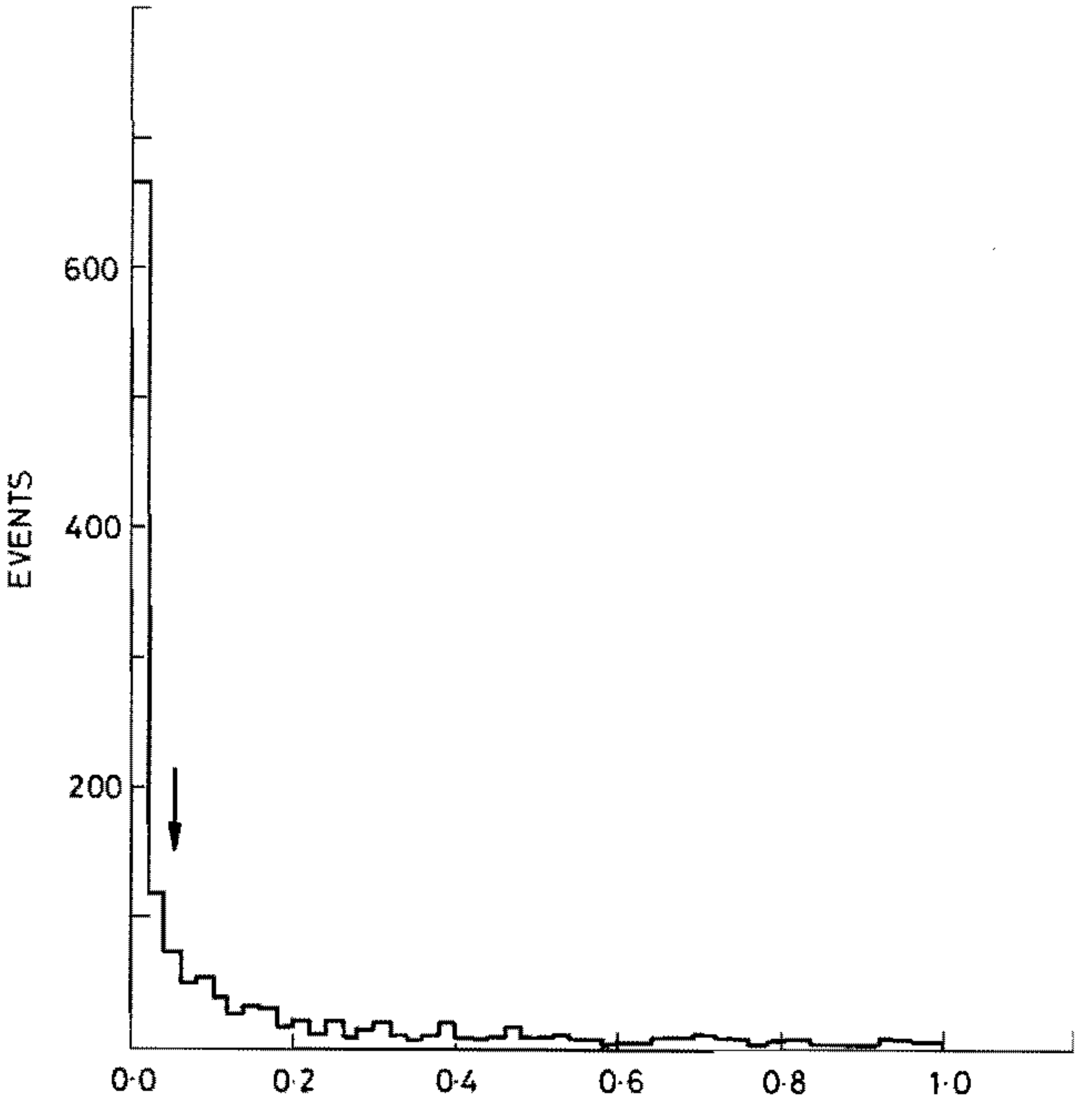

FIG. 4

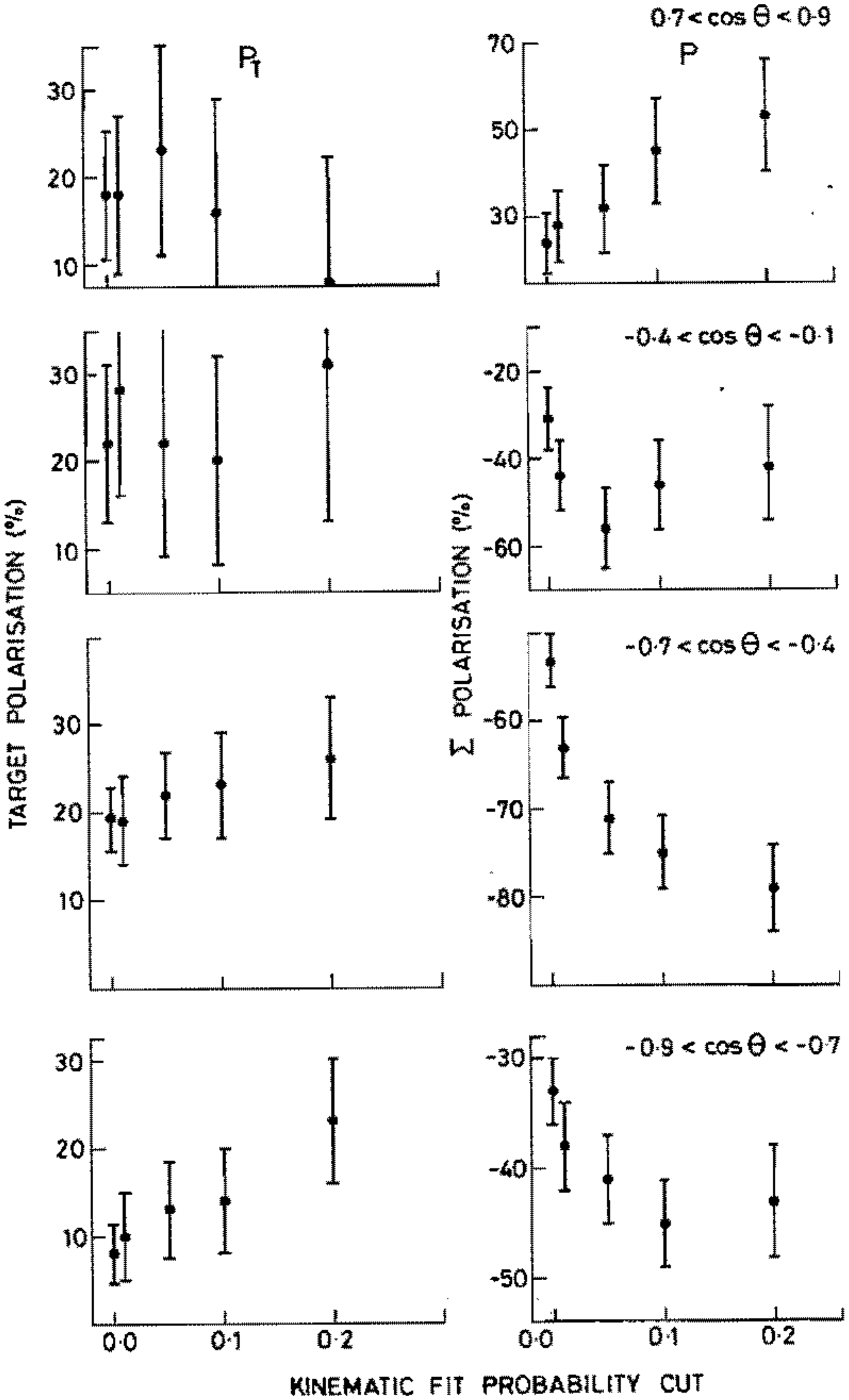

P_T
P
0·7 < cos θ < 0·9
-0·4 < cos θ < -0·1
-0·7 < cos θ < -0·4
-0·9 < cos θ < -0·7
TARGET POLARISATION (%)
Σ POLARISATION (%)
KINEMATIC FIT PROBABILITY CUT

FIG. 5

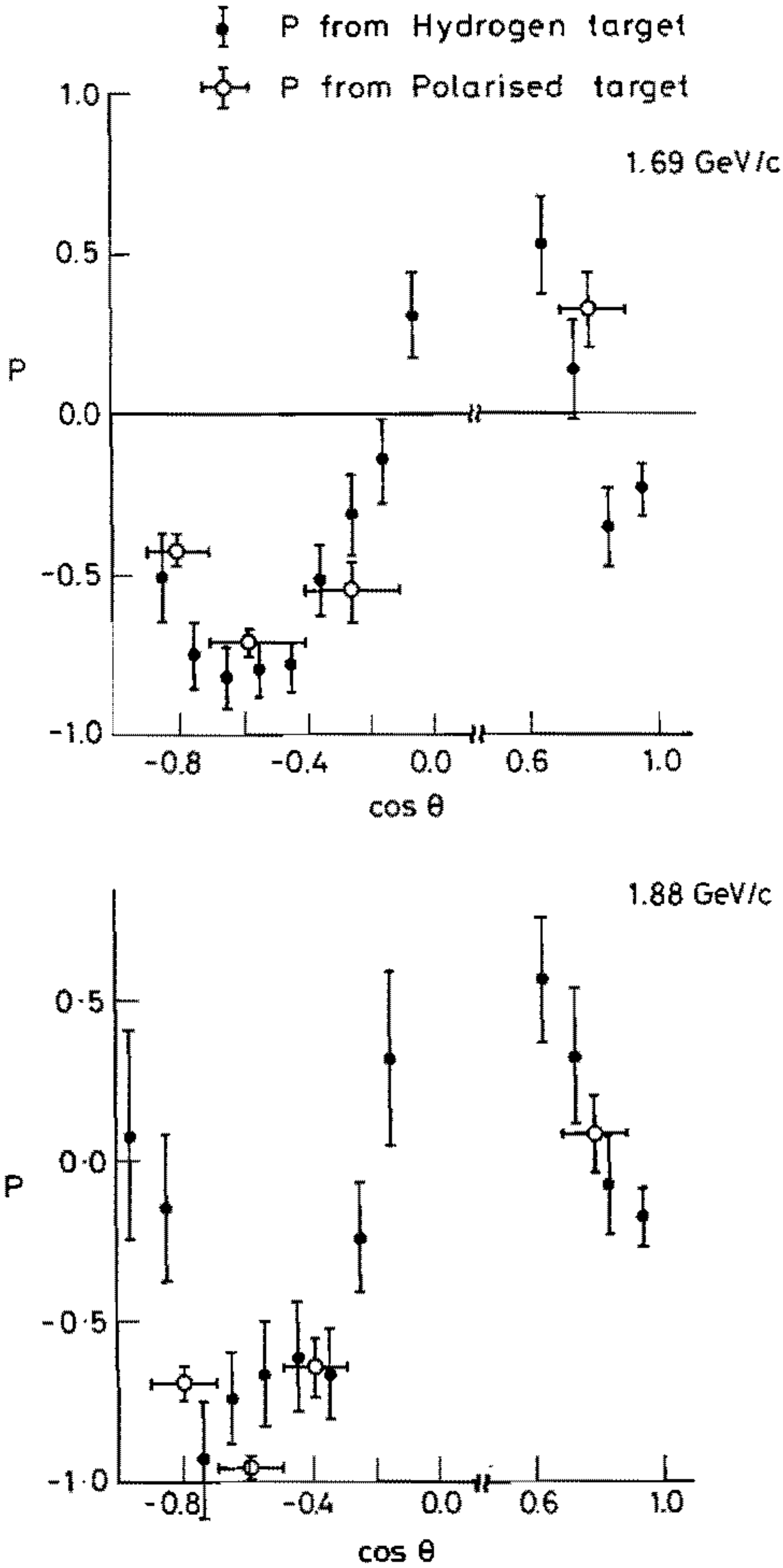

P from Hydrogen target
P from Polarised target
1.69 GeV/c
1.0
0.5
0.0
-0.5
-1.0
P
-0.8
-0.4
0.0
0.6
1.0
cos θ
1.88 GeV/c
0·5
0·0
-0·5
-1·0
P
-0.8
-0.4
0.0
0.6
1.0
cos θ

FIG. 6

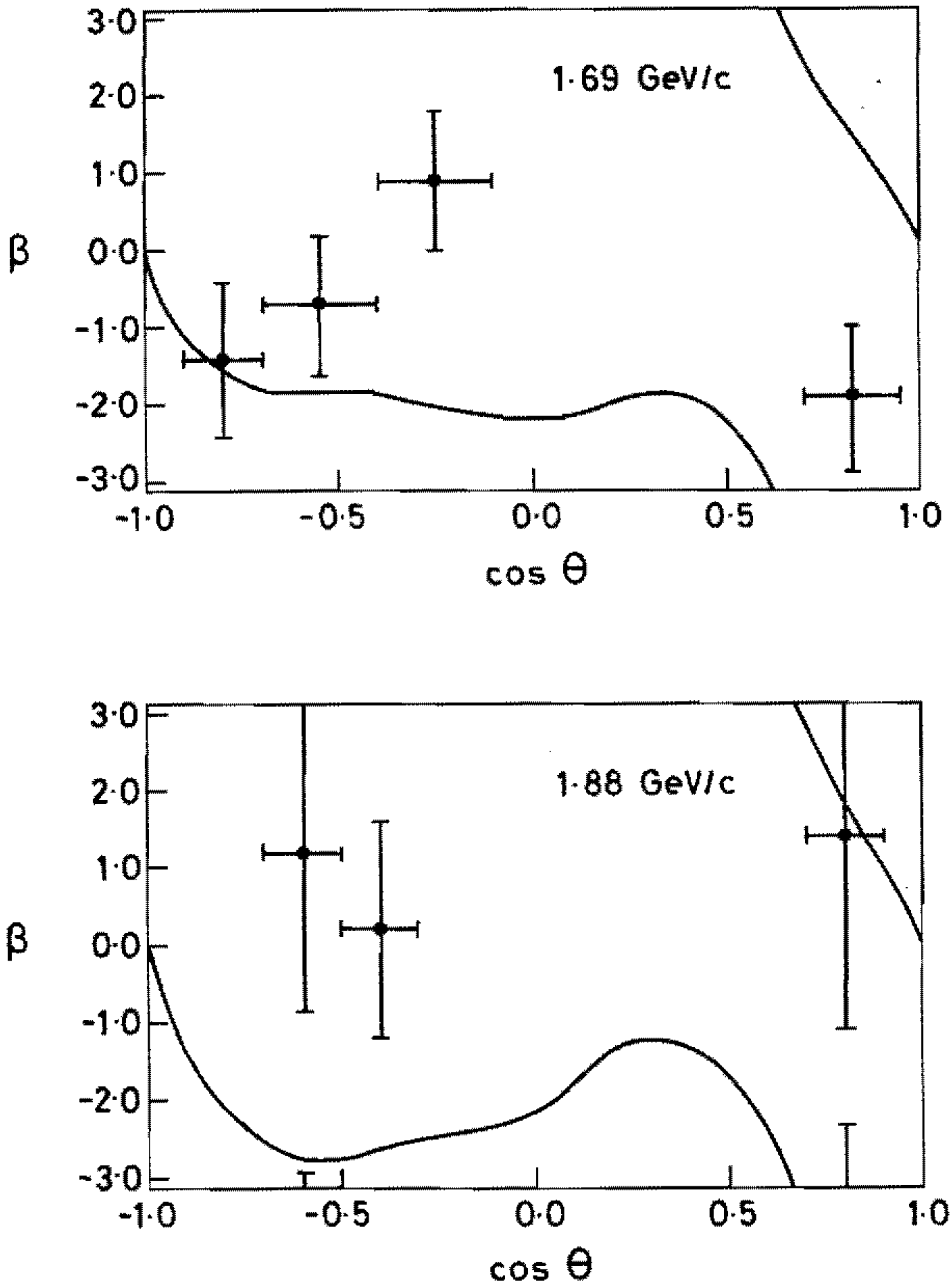
1·69 GeV/c
β
3·0
2·0
1·0
0·0
-1·0
-2·0
-3·0
-1·0
-0·5
0·0
0·5
1·0
cos θ
1·88 GeV/c
β
3·0
2·0
1·0
0·0
-1·0
-2·0
-3·0
-1·0
-0·5
0·0
0·5
1·0
cos θ

FIG· 7

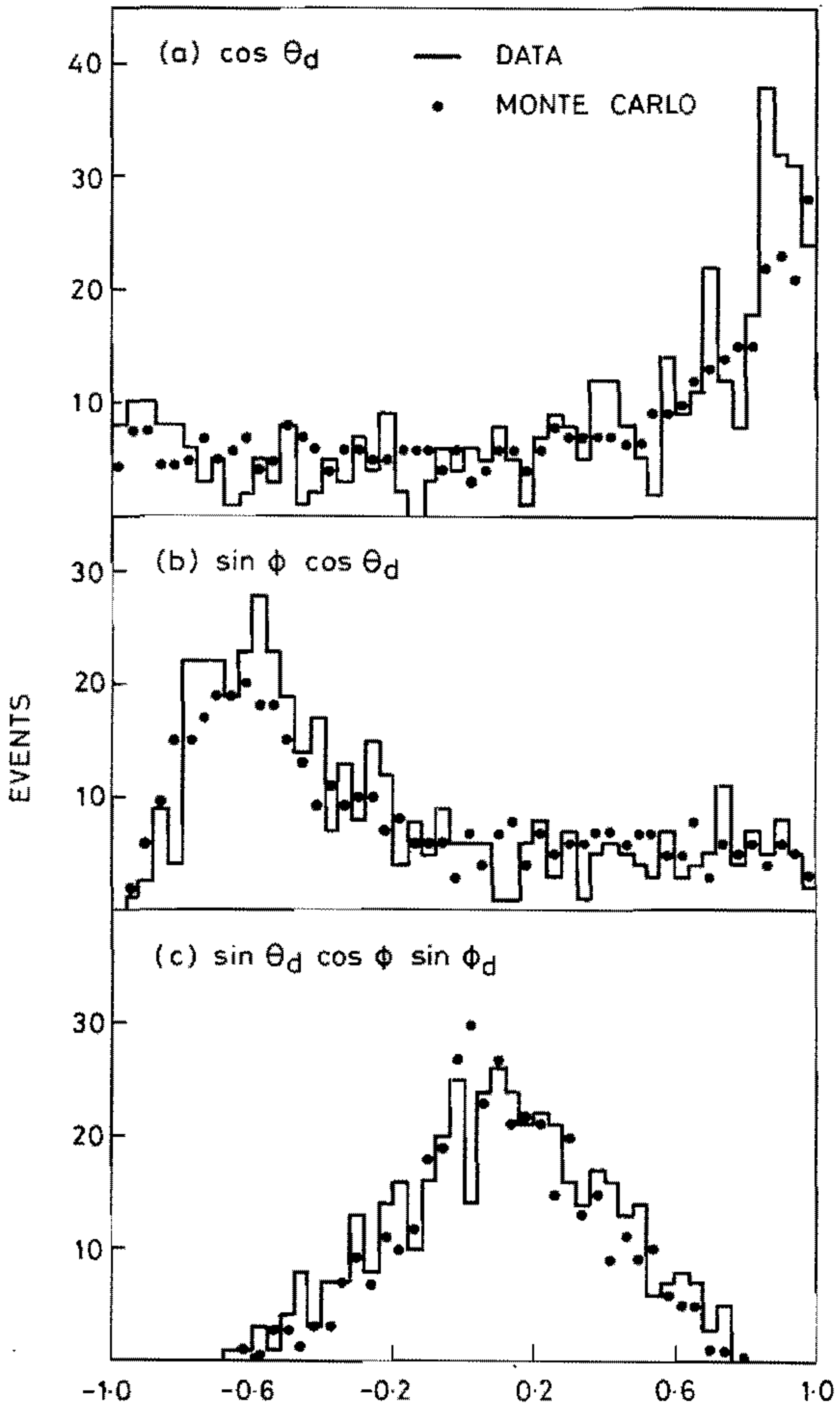

(a) cos θd
DATA
MONTE CARLO
(b) sin φ cos θd
(c) sin θd cos φ sin φd
EVENTS
40
30
20
10
-1·0
-0·6
-0·2
0·2
0·6
1·0

FIG. 8